

Comparative assessment of the dynamic behaviour of an exothermal chemical reaction including data uncertainties

Ulrich Hauptmanns*

Abteilung Anlagentechnik und Anlagensicherheit, Otto-von-Guericke-Universität Magdeburg, Universitätsplatz 2, D-39106 Magdeburg, Germany

Received 30 March 2007; received in revised form 13 September 2007; accepted 19 September 2007

Abstract

The prediction of the dynamic behaviour of a chemical process is important for reactor design, optimization and safety. It is, however, beset with uncertainties of both, models and their input data. The latter are addressed here and the influence of uncertainties of key parameters, i.e. the heat of reaction, the reaction rate constant and the apparent energy of activation, on the calculation results and the conclusions drawn from them is shown. The conventional approach for the propagation of uncertainties through calculations, the Monte-Carlo method, is compared with calculations using polynomial chaos. The latter require considerably less time for calculation and are hence better suited for parameter variations, which are always needed in the design process. Both approaches are applied to an existing plant for manufacturing the explosive hexogen and illustrated by showing the evolution of the concentration of the product with time and the associated uncertainties. The ranges of predicted production quantities and raw material consumption as well as the impact of uncertainties on designing the dumping system for preventing a runaway reaction after cooling failure are also presented.

© 2007 Published by Elsevier B.V.

Keywords: Monte-Carlo; Polynomial chaos; Exothermal reactions; Hexogen

1. Introduction

Uncertainties in engineering calculations affect both, models and their input data. The latter are addressed here. Among the sources of data uncertainties figure the following (cf. [1]):

1. systematic error (due to biases in measuring apparatuses and experimental procedures);
2. transfer of data measured in a specific environment (e.g. laboratory) to industrial conditions;
3. insufficient knowledge (due to economic or other constraints);
4. random errors and unavoidable statistical variations (due to unavoidable imperfections in measurement);
5. variability (due to fluctuations of a quantity with time, e.g. heat transfer coefficient owing to instabilities of flow);
6. inherent randomness (as a consequence of the Heisenberg indeterminacy).

Whilst the uncertainties due to lack of knowledge, also called epistemic, i.e. (1)–(3), may be reduced, although the effort required may be an obstacle, stochastic uncertainties, i.e. (4)–(6), will always be present. Both types of uncertainties are usually described by probability distributions.

Lack of knowledge concerning data for chemical reactor calculations can manifest itself by their dearth or even absence, so that (uncertain) analogies, expert judgment and the like have to be used. Uncertainty may also result from the co-existence of several different data for the same parameter, each of which potentially applies to the problem at hand.

The relevance of uncertainties stems from their impact on simulation results. They affect the design and optimization of a system and, in particular, the design of safety-relevant features. If not heeded, over or underdesign may be the consequence. In addition, taking into account uncertainties enables one to accommodate the fact that different input data are normally known with different degrees of certainty, a circumstance which should be reflected by the calculation results. Furthermore, the systematic analysis of uncertainties can provide insight into the level of confidence of model estimates and help identify key sources of uncertainties [2]. Data uncertainties have been a concern in the optimization of process

* Tel.: +49 391 6718831; fax: +49 391 6711128.

E-mail address: ulrich.hauptmanns@vst.uni-magdeburg.de.

plants (cf. [3–6]) but less so in relation with plant safety (cf. [7,8]).

In order to assess the impact of input data uncertainties on the results they have to be propagated through the calculations. This propagation is usually performed using the Monte-Carlo method, either in its straight form or applying effort-reducing techniques such as Latin Hypercube Sampling (cf. [9]). In any case, heavy computational demand results.

Alternatives which reduce this demand are the stochastic response surface method whose application to chemical reaction systems is explored in [2] and a non-stochastic approach known as homogeneous polynomial chaos. It is founded on the homogeneous chaos theory [10]. Uncertainty is treated there by a spectral expansion based on Hermite orthogonal polynomials in terms of Gaussian random variables. This method was applied extensively to problems in mechanics (cf. [11]).

Application of the straight Monte-Carlo method to chemical processes is found in [6] and [7], that of the Latin Hypercube Procedure in [8]. The treatment of uncertainties affecting chemical process simulations by means of the polynomial chaos approach is presented in [12] and [13].

The purpose of the present paper is to show the impact of uncertainties on the analysis of a chemical process as well as the design considerations derived therefrom and to compare the Monte-Carlo and polynomial chaos approaches. This is done by analyzing the dynamic behaviour of the process step “nitration” of an existing plant for the production of the explosive hexogen as a typical example of an exothermal process.

This process would require the reactor to be tripped by dumping its contents into a knock-out tank in case a runaway reaction should occur. In this context the influence of uncertainties on assessing the time available for the trip is shown.

The paper is organized as follows: the example process and the derivation of the kinetic equation is described in Section 2 followed by the process model in Section 3. The treatment of the

Table 1
Operational parameters of the nitration reactor

Parameter	Symbol	Datum
Volume of the reaction zone	V	630 l
Initial temperature of reaction	$T(0)$	4.0 °C
Mass of reactor contents	–	970.2 kg
Volumetric flow through the reactor	\dot{V}	0.49 l/s
Concentration of hexamine in feed	$C_{HA,in}$	0.9851 mol/l
Concentration of nitric acid in feed	$C_{HNO_3,in}$	20.9087 mol/l
Coolant inlet temperature	$T_{c,in}$	–5.0 °C
Area of the heat exchanger (jacket and coil inside)	F	7.0 m ²
Global heat transfer coefficient	U	1.4 kW/(m ² K)
Specific heat capacity of the coolant (water plus 25% of methanol)	$c_{p,c}$	3.6 kJ/(kg K)

uncertain quantities, i.e. heat of reaction and the kinetic parameters, is dealt with in Section 4 and their propagation through the calculation by both, Monte-Carlo and polynomial chaos, is treated in Section 5. Section 6 is devoted to a comparison of the results. Times available for trip are discussed in Section 7 and the conclusions are drawn in Section 8.

2. Process description and reaction kinetics

The production of the explosive hexogen, also known as RDX, is described in detail in [14]. The plant considered employs the so-called SH process, in which hexamethylenetetramine (hexamine) reacts with nitric acid to form RDX. Its fundamental step, the nitration, is analysed in more detail below.

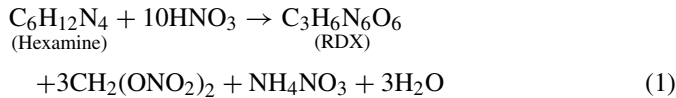
The reaction takes place in a continuously stirred tank reactor, which forms part of a cascade of reactors. An excess of nitric acid by a factor between 8 and 10, as well as reaction temperatures below 20 °C are required for safe operation. The reaction is started by feeding hexamine via a transportation screw into

Table 2
Physical properties and feed temperatures of the substances involved in the nitration process

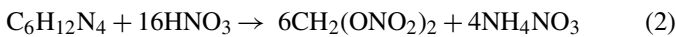
Area	Datum			
Feed	Hexamine C ₆ H ₁₂ N ₄	Molar mass	M_{HA}	140.19 kg/kmol
		Heat capacity	$c_{p,HA}$	1.256 kJ/(kg K)
		Temperature	$T_{HA,in}$	20 °C
Nitric acid HNO ₃	Nitric acid HNO ₃	Molar mass	M_{HNO_3}	63.01 kg/kmol
		Heat capacity	c_{p,HNO_3}	1.989 kJ/(kg K)
		Concentration	–	Approximately 98.5%
		Temperature	$T_{HNO_3,in}$	4 °C
Products and side products	Hexogen C ₃ H ₆ N ₆ O ₆	Molar mass	M_{RDX}	222.12 kg/kmol
		Heat capacity	$c_{p,RDX}$	1.19 kJ/(kg K)
Methanediol dinitrate CH ₂ (ONO ₂) ₂	Methanediol dinitrate CH ₂ (ONO ₂) ₂	Molar mass	M_C	138.04 kg/kmol
		Heat capacity	$c_{p,C}$	1.926 kJ/(kg K)
Ammonium nitrate NH ₄ NO ₃	Ammonium nitrate NH ₄ NO ₃	Molar mass	M_D	80.05 kg/kmol
		Heat capacity	$c_{p,D}$	1.759 kJ/(kg K)
Water H ₂ O	Water H ₂ O	Molar mass	M_{H_2O}	18 kg/kmol
		Heat capacity	c_{p,H_2O}	4.187 kJ/(kg K)

the reactor, which is filled with nitric acid at 4 °C. Operational details of the reactor provided by a manufacturer are given in Table 1.

Several reactions take place concurrently. The complex reaction network can be described by the following simplified set of reaction equations (cf. [15]).



for the formation of the product and



for the side reaction. Since no details about the kinetics of the side reaction are available, the following treatment will, of necessity, be limited to the main reaction.

The physical properties of the substances needed for the calculations are given in Table 2.

The nitration process is exothermal. Different heats of nitration are quoted, i.e. 162.5 kJ, 293.4 kJ, 368.3 kJ per mol of nitrated hexamine [14]. The heat of nitration, $-\Delta H_r$, must therefore be considered as an uncertain datum (epistemic uncertainty). On the other hand, the data provided in [14] are insufficient for deriving a temperature-dependent kinetic equation. Such an equation may be obtained, within narrow limits, from experimental evidence presented in [15], which is given in Table 3 along with conversion rates calculated using the equations stated below.

The rate of the nitration reaction is given by

$$\begin{aligned} r(t, T) &= k_R(T) C_{\text{HNO}_3}^0 C_{\text{HA}}(t)^n \\ &= A \exp\left(-\frac{ER}{T}\right) C_{\text{HNO}_3}^0 C_{\text{HA}}(t)^n \end{aligned} \quad (3)$$

where $r(t, T)$ is the reaction rate, A the pre-exponential factor, E the apparent energy of activation, R the gas constant, n the order of reaction and T is the temperature.

Since the experiment was conducted with an excess of nitric acid (weight ratio 11:1) its concentration, $C_{\text{HNO}_3}^0$, is considered as constant in time. The depletion of hexamine is then governed

by

$$\frac{dC_{\text{HA}}}{dt} = -A \exp\left(-\frac{E}{RT}\right) C_{\text{HNO}_3}^0 C_{\text{HA}}(t)^n \quad (4)$$

Considering that $C_{\text{HA}}(t) = C_{\text{HA}}^0 [1 - x_A(t)]$ the solution of Eq. (4) may be written as

$$\ln \left[\frac{t}{[1 - x_A(t)]^{1-n} - 1} \right] = \ln \left[\frac{(C_{\text{HA}}^0)^{1-n}}{A(n-1)C_{\text{HNO}_3}^0} \right] + \frac{E}{RT} \quad (5)$$

which lends itself to linear regression analysis in the form

$$\ln \left[\frac{t}{[1 - x_A(t)]^{1-n} - 1} \right] = \mu_a + \frac{\mu_b}{T} \quad (6)$$

in order to obtain the parameters E , A and n of Eq. (3).

The resulting regression coefficients are $\mu_a = -25.962$ with a standard deviation of $\sigma_a = 1.782$ and $\mu_b = 4136.5$ with a standard deviation of $\sigma_b = 491.11$. Since both coefficients stem from the same set of experimental values, they are correlated, the correlation coefficient ρ being -0.99774 .

Considering that in the experiment the initial concentrations were $C_{\text{HNO}_3}^0 = 21.388$ mol/l and $C_{\text{HA}}^0 = 0.888$ mol/l one obtains, by combining Eqs. (5) and (6), $E = \mu_b R = 34.3909$ kJ/mol, $A = \exp(-\mu_a/\gamma) = 2,850,288,090$ (l/mol)^{9.958} min⁻¹ = 47,504,801 (l/mol)^{9.958} s⁻¹ with $n = 9.958$ (the latter was found by varying n and choosing the value providing the best fit), where $\gamma = C_{\text{HNO}_3}^0 (n-1) C_{\text{HA}}^{0n-1}$.

Table 3 shows that the agreement between the experimental and calculated values within the range of interest for the present analysis of the dynamic behaviour of the reactor, viz. 0–23 °C, is excellent. The quality in describing the experimental values for 0 °C cited in [14] warrants the application of the equation to the concentration of nitric acid in the present process, viz. 98.5%, especially for longer times of residence, as can be seen from Table 4.

3. Basic process model

Based on Eq. (1) the following dynamic model for the reaction may be formulated. It makes use of the concept of the continuously stirred tank reactor (CSTR) (cf. [16]).

Table 3
Observed fractional conversions of the nitration of hexamine to hexogen for different temperatures and times of residence with nitric acid of 98% (bold numbers: values used for determining the kinetic parameters)

Temperature in °C	Reaction time in min	Fractional conversion of hexamine (observed) x_A	Fractional conversion of hexamine (calculated)
-25	600	0.83	0.83
-10	360	0.83	0.83
0	120	0.82	0.82
10	45	0.82	0.82
20	15	0.81	0.80
30	10	0.80	0.80
35	19	0.80	0.82
40	5	0.79	0.80
50	5	0.73	0.81
60	5	0.63	0.82

Table 4

Observed fractional conversions of the nitration of hexamine to hexogen at 0 °C for different times of residence and concentrations of nitric acid

Time in min	Concentration of HNO ₃ (fractional conversion of hexamine (observed) x_A)		Fractional conversion of hexamine (calculated)
	99%	96%	
1.5	–	0.557	0.714
2.5	0.669	0.687	0.730
6.5	0.702	0.753	0.757
12	0.746	0.747	0.774
24	0.809	0.792	0.790
50	0.805	–	0.807

3.1. Process model

- Hexamine (HA)

$$V \frac{dC_{HA}}{dt} = \dot{V}C_{HA,in} - \dot{V}C_{HA} - Vr(t, T), \quad C_{HA}(0) = 0 \quad (7)$$

- Nitric acid (HNO₃)

$$V \frac{dC_{HNO_3}}{dt} = \dot{V}C_{HNO_3,in} - \dot{V}C_{HNO_3} - 10Vr(t, T), \quad C_{HNO_3}(0) = 20.91 \quad (8)$$

- Hexogen (RDX)

$$V \frac{dC_{RDX}}{dt} = -\dot{V}C_{RDX} + Vr(t, T), \quad C_{RDX}(0) = 0 \quad (9)$$

- Methanediol dinitrate (C)

$$V \frac{dC_C}{dt} = -\dot{V}C_C + 3Vr(t, T), \quad C_C(0) = 0 \quad (10)$$

- Ammonia nitrate (D)

$$V \frac{dC_D}{dt} = -\dot{V}C_D + Vr(t, T), \quad C_D(0) = 0 \quad (11)$$

- Water (H₂O)

$$V \frac{dC_{H_2O}}{dt} = -\dot{V}C_{H_2O} + 3Vr(t, T), \quad C_{H_2O}(0) = 0 \quad (12)$$

3.2. Process energy balance

$$\sum_{i=1}^6 C_i M_i c_{p,i} V \frac{dT}{dt} = \dot{Q} - \dot{Q}_{cool}, \quad T(0) = 277.16 \quad (13)$$

where $\dot{Q} = \dot{V}(C_{HA,in}M_{HA}c_{p,HA}T_{HA,in} + C_{HNO_3,in}M_{HNO_3}c_{p,HNO_3}T_{HNO_3,in} - \sum_{i=1}^6 C_i M_i c_{p,i}T) + (-\Delta H_r)r(t, T)V$ denotes the heat generated and $\dot{Q}_{cool} = \dot{m}c_{p,c}(T - T_{c,in})[1 - \exp(-FU/\dot{m}c_{p,c})]$ the heat extracted, with i denoting the above mentioned substances (HA, HNO₃, RDX, C, D, H₂O).

3.3. PI controller for coolant flow

$$\frac{d\dot{m}}{dt} = \frac{K_1}{\tau}(\dot{Q} - \dot{Q}_{cool}) + \frac{K}{\tau}s_h, \quad \dot{m}(0) = 2 \quad (14)$$

$$\frac{ds_i}{dt} = \frac{K_{mV/T}T - u_c}{p_i}, \quad s_i(0) = 0 \quad (15)$$

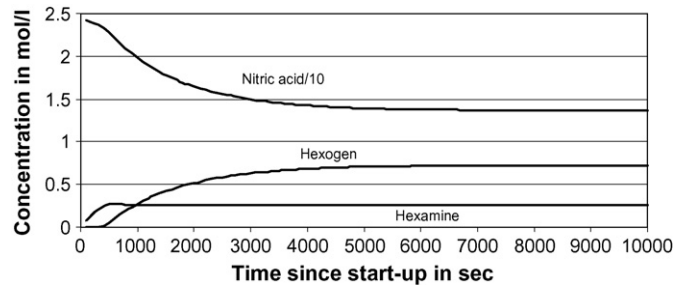


Fig. 1. Evolution of the concentrations of the principal substances with time (calculated with point values).

$$s_h = u_c - K_{mV/T}T + s_i, \quad s_h(0) = 0 \quad (16)$$

In Eqs. (14)–(16) \dot{m} in kg/s is the mass flow of coolant, $K_1 = 1$ kg/kW, $K = 200$ kg/mV the cooler gain, $\tau = 2000$ s the cooler time constant, $p_i = 4000$ s the integrator coefficient, $u_c = 288.16$ mV the command signal and $K_{mV/T} = 1.0$ mV/K is the gain in mV in the transducer.

The system is solved using a Runge-Kutta algorithm with an adaptive time step size. The evolution of the concentrations of the principal substances involved in the process with time is found in Fig. 1. The calculations are based on mean values (point values).

Relevant parameters for the process at steady state are presented in Table 5.

4. Uncertainties

All parameters involved in the process are beset with uncertainties. Major impacts are to be expected from the uncertainties affecting the heat of reaction, the reaction rate constant and the apparent energy of activation. As usual, these quantities are rep-

Table 5
Process parameters at steady state (calculations with point values)

Parameter	Quantity
Hexamine feed	243.60 kg/h
Hexamine discharge	64.09 kg/h
Nitric acid feed	2323.99 kg/h
Nitric acid discharge	1517.12 kg/h
Hexogen production	284.47 kg/h
Hexamine consumption per 1 t of hexogen	631.06 kg/t
Nitric acid consumption per 1 t of hexogen	2836.37 kg/t
Temperature of production	15.67 °C

resented by probability distributions. In the case of the heat of reaction the Weibull distribution (cf. [17]) was chosen from among seven different probability distributions, since it produced the smallest quadratic deviation. The Weibull probability density function is

$$f_{\Delta H}(|\Delta H_r|) = \eta b (\eta |\Delta H_r|)^{b-1} \exp(-\eta |\Delta H_r|^b),$$

$$|\Delta H_r|, b, \eta > 0 \quad (17)$$

The corresponding parameter values are: $b=3.85$ and $\eta=0.003274$.

The uncertainties of the regression coefficients are supposed, as usual, to be binormally distributed. Hence, the regression estimators a and b are represented by a bivariate normal distribution with probability density function (cf. [17])

$$f_{A,B}(a, b) = \frac{\exp \left\{ -\frac{1}{2(1-\rho^2)} \left[\frac{(a-\mu_a)^2}{\sigma_a^2} - 2\rho \frac{(a-\mu_a)(b-\mu_b)}{\sigma_a\sigma_b} + \frac{(b-\mu_b)^2}{\sigma_b^2} \right] \right\}}{2\pi\sigma_a\sigma_b\sqrt{1-\rho^2}},$$

$$0 \leq a, b < \infty; \sigma_a, \sigma_b > 0; |\rho| < 1 \quad (18)$$

with the mean values, standard deviations and correlation coefficient stated in Section 2.

5. Uncertainty propagation

If the uncertainties represented by Eqs. (17) and (18) are taken into consideration, Eqs. (7)–(16) become a system of stochastic differential equations. In what follows this will be solved using the Monte-Carlo and the polynomial chaos approaches.

5.1. Monte-Carlo

The Monte-Carlo approach entails the generation of a large number of realizations from the probability distributions for the uncertain quantities involved, viz. Eqs. (17) and (18), and the solution of the system of deterministic equations describing the process with the input data from every set of the realizations. Every calculation is called a trial. The trials result in a probability distribution of the final result for the parameter in question, e.g. concentrations, production temperature, etc., which are normally described by their means, variances and percentiles. This probability distribution reflects the impact of the uncertainties of the input data on the calculation results.

The major disadvantage of the method is its $1/\sqrt{P}$ convergence, with P being the number of trials. This leads to a considerable calculational effort, which, depending on the complexity of the underlying system of equations, may become prohibitive.

The realizations from Eqs. (17) and (18) are obtained by generating in the first place random numbers uniformly distributed on $[0,1]$ and then transforming them into the pertinent distributions. If $Z_p, Z_{p,1}, \dots, Z_{p,4}$ ($p=1, \dots, P$ denotes the p th trial) represent these uniform random numbers the following transformations produce the required results

- Weibull distribution

$$|\Delta H_{r,p}| = \frac{-\ln Z_p}{\eta} \quad (19)$$

- Bivariate normal distribution

$$U_p = \sqrt{-2 \ln Z_{p,1}} \cos(2\pi Z_{p,2}),$$

$$V_p = \sqrt{-2 \ln Z_{p,3}} \cos(2\pi Z_{p,4}),$$

$$A_p = U_p \sigma_a + \mu_a \quad \text{and}$$

$$B_p = \left(\rho U_p + \sqrt{(1-\rho^2)} V_p \right) \sigma_b + \mu_b \quad (20)$$

A_p and B_p are the realizations of the coefficients a and b of Eq. (18).

The uniformly distributed random numbers were generated using L'Ecuyer's algorithm (cf. [18]).

As an example the evolution of the hexogen concentration as a function of time after start-up (the process is shut down every weekend) is shown in Fig. 2. The differences between the 5th and 95th centiles are obvious. They would lead to a prediction of the stationary hourly production of hexogen between 279.28 and 287.14 kg.

5.2. Polynomial chaos

Given the slow convergence of the Monte-Carlo method an alternative, the spectral expansion of uncertainties based on Hermite orthogonal polynomials (cf. [19]) in terms of Gaussian random variables with mean 0 and variance 1 (cf. [20]), is presented here. It provides a means of expanding second order random processes in terms of orthogonal polynomials. Such processes are characterized by having a finite variance, a requirement satisfied by most physical processes. Details are presented in what follows.

Let

$$\frac{dy}{dt} = -\alpha y + d \quad (21)$$

represent any one of Eqs. (7)–(13), where α and d are the random quantities.

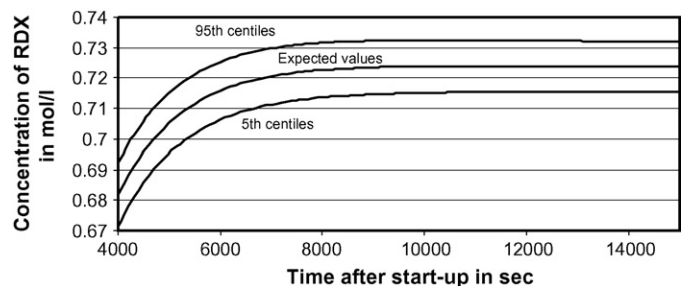


Fig. 2. Evolution of the concentration of hexogen with time including uncertainty ranges calculated by the Monte-Carlo method (10,000 trials).

Table 6
Details of polynomial chaos (according to [11])

k	k th polynomial chaos	$\langle \Phi_k^2 \rangle$
0	1	1
1	ξ	1
2	$\xi^2 - 1$	2
3	$\xi^3 - 3\xi^2$	6
4	$\xi^4 - 6\xi^2 + 3$	24

The polynomial chaos expansion then consists in setting

$$y(t) = \sum_{k=0}^K y_k(t) \Phi_k(\xi); \quad \alpha = \sum_{k=0}^K \alpha_k \Phi_k(\xi);$$

$$d = \sum_{k=0}^K d_k \Phi_k(\xi) \tag{22}$$

where ξ is a random variable and $\Phi_k(\xi)$ the polynomial chaos of order k (Hermite's polynomials in the present case). Introduction of Eq. (22) into Eq. (21) gives

$$\sum_{k=0}^K \frac{dy_k(t)}{dt} \Phi_k(\xi) = - \sum_{k=0}^K \sum_{j=0}^K y_k(t) \Phi_k(\xi) \alpha_j \Phi_j(\xi)$$

$$+ \sum_{k=0}^K d_k \Phi_k(\xi) \tag{23}$$

The polynomials form an orthogonal basis with respect to the weight function $\exp(-\xi^2/2)/\sqrt{2\pi}$, so that multiplication of Eq. (23) by $\Phi_l \exp(-\xi^2/2)/\sqrt{2\pi}$ and integration over the domain of definition, i.e. $-\infty, \infty$, denoted by $\langle \cdot \rangle$ leads to

$$\frac{dy_l(t)}{dt} = - \frac{1}{\langle \Phi_l^2 \rangle} \left(\sum_{k=0}^K \sum_{j=0}^K y_k(t) \alpha_j e_{k,j,l} \right)$$

$$+ d_l, \quad l = 0, \dots, K \tag{24}$$

where $e_{k,j,l} = \langle \Phi_k \Phi_j \Phi_l \rangle$ is readily evaluated using the relations

$$E \xi^{2k+1} = 0, \quad E \xi^{2k} = \frac{(2k)!}{2^k k!}$$

$$\text{with } E \xi^k = \frac{1}{\sqrt{2\pi}} \int_{-\infty}^{\infty} \xi^k \exp\left(-\frac{\xi^2}{2}\right) d\xi \tag{25}$$

In the present case one-dimensional chaos is appropriate, because the deviation of the process from Gaussian behaviour is small. In such a case exponential convergence has been proved [21]. Hence, an order of $K=4$ ensured sufficient convergence of the series of Eq. (22), which were therefore truncated with the fifth term. Table 6 shows the polynomials and their orthogonality properties.

Cases of strong deviations from Gaussian behaviour may be treated by increasing the number of dimensions or applying generalized polynomial chaos, where polynomials other than Hermite's are used. Strong non-linearities may require an increased order of polynomials (cf. [22]). All of this, just as when a high number of reactions must be considered would

lead to an increase in the number of simultaneous non-linear equations to be solved. In particular a system of L simultaneous, in general coupled, first order differential equations would have to be solved, where

$$L = \frac{(K+N)!}{K!N!} M \tag{26}$$

with polynomial order K , dimension N and number of process equations M . It is obvious that L might become prohibitively large, if all parameters have to be increased at the same time. The advantages over the Monte-Carlo method may then be lost.

The above procedure was applied to Eqs. (7)–(13) using the stochastic coefficients whose derivation is described below. The system of seven stochastic equations is thus converted into a system of $L=35$ deterministic equations which was solved by the Runge-Kutta algorithm already mentioned.

If y is a random variable with a continuous distribution function $G(y)$ and probability density function $g(y)$ which satisfies

$$G(y) = \int_{-\infty}^y g(y') dy' \tag{27}$$

and $\{\Phi(\xi)\}$ a set of polynomial chaos whose underlying random variable ξ has the distribution function $F(\xi)$ and probability density function $f(\xi)$ such that

$$F(\xi) = \int_{-\infty}^{\xi} g(\xi') d\xi' \tag{28}$$

then the representation of y takes the form (cf. [20])

$$y = \sum_{k=0}^K y_k \Phi_k(\xi), \quad \text{where } y_k = \frac{\langle y, \Phi_k(\xi) \rangle}{\langle \Phi_k^2(\xi) \rangle} \tag{29}$$

Evaluation of the numerator $\langle \cdot \cdot \rangle$ needs caution because in most cases y and ξ belong to different probability spaces. In order to circumvent this difficulty y and ξ are mapped to the probability space defined by the uniform random variable $u \in [0,1]$, i.e.

$$y = G^{-1}(u) \quad \text{and} \quad \xi = F^{-1}(u) \tag{30}$$

Hence we have

$$y_k = \frac{\langle y, \Phi_k(\xi) \rangle}{\langle \Phi_k^2(\xi) \rangle} = \frac{1}{\langle \Phi_k^2(\xi) \rangle} \int_0^1 G^{-1}(u) \Phi_k [F^{-1}(u)] du,$$

$$k = 0, 1, \dots, K \tag{31}$$

In the present case F is the standard normal distribution, whose inverse F^{-1} is readily calculated with a pertinent approximation (cf. [19]).

The integral in Eq. (31) is evaluated using a 10-point Gauss–Legendre quadrature.

- Heat of reaction

The above relationships are evaluated by using Eq. (19) to achieve the transform to $[0,1]$

$$y = G^{-1}(u) = \frac{(-\ln u)^{1/b}}{\eta} \tag{32}$$

- Reaction rate constant

Table 7

Comparison of the reaction rate constants velocities $k_R(T)$ and their variances obtained by Monte-Carlo and polynomial chaos

Temperature in °C	Monte-Carlo (5,000,000 trials)		Polynomial chaos	
	Expected value	Variance	Expected value	Variance
0	12.6865	2.3880	12.6866	2.3639
15	27.9774	15.7349	27.9776	15.5973
30	57.4832	133.3266	57.4829	131.7854

The kinetic equation requires special treatment. Based on Eqs. (5), (6) and (20) the reaction rate equation is decomposed into the following two independent parts:

$$y_1 = G_1^{-1}(u) = \exp \left[-u\sigma_a - \mu_a - \frac{\rho u \sigma_b}{T} \right] \frac{1}{\gamma} \quad (33)$$

$$y_2 = G_2^{-1}(u) = \exp \left[\frac{-\sqrt{1 - \rho^2 u \sigma_b} - \mu_b}{T} \right] \quad (34)$$

The procedure described by Eq. (31) is applied separately to Eqs. (33) and (34). The following results are obtained:

$$E k_R(T) = y_{1,0} y_{2,0} \quad (35)$$

for the expected value and

$$\text{Var } k_R(T) = \sum_{k=0}^K y_{1,k}^2 \sum_{k=0}^K y_{2,k}^2 - (y_{1,0} y_{2,0})^2 \quad (36)$$

for the variance. In deriving Eq. (36) the following relationship for calculating the variance of the product of two independent random variables a and b was used [23].

$$\begin{aligned} \sigma_{a,b}^2 &= E(a^2 b^2) - (Ea)^2 (Eb)^2 = Ea^2 Eb^2 - (Ea)^2 (Eb)^2 \\ &= \left[(Ea)^2 + \sigma_a^2 \right] \left[(Eb)^2 + \sigma_b^2 \right] - (Ea)^2 (Eb)^2 \\ &= \sigma_a^2 \sigma_b^2 + (Eb)^2 \sigma_a^2 + (Ea)^2 \sigma_b^2 \end{aligned} \quad (37)$$

The result is represented by a normal distribution with the expected value calculated according to Eq. (35) and the variance according to Eq. (36). Its representation by polynomial chaos follows the above procedure.

A comparison of the results obtained with this procedure and the corresponding Monte-Carlo simulation presented in Table 7 shows that this approximate approach is feasible for

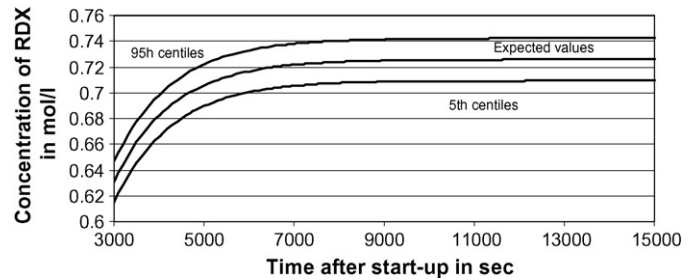


Fig. 3. Evolution of the concentration of hexogen with time including uncertainty ranges calculated by polynomial chaos.

the problem at hand, the maximum deviation (variance for 30 °C) being approximately 1%.

• Reaction rate

Applying the above approach to the constant of reaction the rate of reaction (cf. Eq. (3)) is calculated as follows

$$\begin{aligned} k_R &= \frac{1}{\langle \Phi_k^2(\xi) \rangle} \int_0^1 k_R^{-1}(u) \Phi_k \left[F^{-1}(u) \right] \\ &\quad \times \left(\sum_{l=1}^K C_{HA,l} \Phi_l \left[F^{-1}(u) \right] \right)^n \\ &\quad \sum_{l=1}^K C_{HNO_3,l} \Phi_l \left[F^{-1}(u) \right] du, \quad k = 0, 1, \dots, K \end{aligned} \quad (38)$$

where $k_R^{-1}(u)$ is the inverse of a normal distribution with the expected value from Eq. (35) and variance from Eq. (36). $C_{HA,l}$, $C_{HNO_3,l}$ are the spectral coefficients of the concentrations of hexogen and nitric acid, respectively. The integral in Eq. (38) is evaluated using a 10-point Gauss–Legendre quadrature.

As an example the evolution of the hexogen concentration with time is shown in Fig. 3. The differences between the 5th and 95th centiles are considerable. They would lead to a prediction of the stationary hourly production of hexogen between 277.92 and 290.97 kg.

6. Comparison of results

Key parameters of the process were calculated using both, the Monte-Carlo and polynomial chaos procedures, as well as point values. They are shown in Table 8. In the Monte-Carlo calculations for the steady state the coolant flow was fixed at an average value in order to create the same

Table 8

Some key parameters of the process calculated according to different procedures

Parameter	Point values	Monte-Carlo (10,000 trials)			Polynomial chaos		
		5th	Mean	95th	5th	Mean	95th
Hexamine discharge in kg/h	64.09	62.40	64.88	67.36	59.99	64.10	68.22
Nitric acid discharge in kg/h	1517.12	1509.55	1520.70	1531.84	1498.69	1517.21	1535.72
Hexogen production in kg/h	284.47	279.28	283.21	287.14	277.92	284.44	290.97
Production temperature in °C	15.67	6.70	13.14	19.59	9.04	15.70	22.36

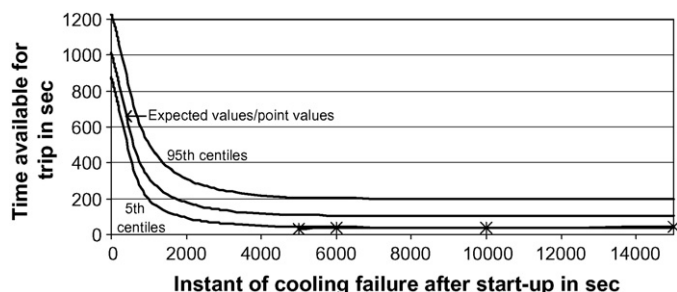


Fig. 4. Time available for reactor trip after cooling failure as a function of the instant of failure calculated with polynomial chaos (point values coincide with the expected values of the polynomial chaos calculations; asterisks: Monte-Carlo calculations).

boundary conditions as for the polynomial chaos, which is essential for comparison. Otherwise the control would try to compensate parameter fluctuations by raising or decreasing coolant flow beyond ranges normally provided for in controls.

The agreement of the mean values is perfect. Polynomial chaos leads to slightly larger uncertainty ranges than Monte-Carlo, the differences lying practically always below 1%.

The calculation times are a few minutes for polynomial chaos as compared with approximately 10 h for Monte-Carlo on the same PC.

7. Assessment of the times available for trip

Should the reactor cooling fail, the reaction temperature would increase with a gradient depending on the status of the reactor at the instant of failure. For such an occurrence a system is provided which would discharge the reactor contents by gravity into a knock-out tank below the reactor. Fig. 4 shows the times which are available for dumping if a maximum temperature of 23 °C is tolerated as a safe distance from runaway. It is obvious that uncertainties affect the prediction, which should, of course, be on the safe side. In the present case a minimum value of the 5th centile of 39.2 s is predicted as compared with 102.9 s if point values are used. In order to ensure a successful functioning the result accounting for uncertainties should be used. Given that the discharge pipe has a diameter of 200 mm, a conservative calculation shows that 15.4 s would be sufficient for complete discharge, leaving the difference in time for the activation of the trip. The above statement means that there is a 95% chance of dumping in time if no more than 39.2 s are needed. It must be kept in mind, however, that these low available times just prevail for about 17.2 h, which are only part of the period of the 120 h of weekly operation. Hence, assuming demands uniformly distributed over the production period there is a probability of 0.14 that a demand on the system takes place during the 17.2 h mentioned. This leads to a probability of failure (assuming the technical components involved work perfectly) of 0.0072. About 20 h after start-up the 5th centile reaches an asymptotic level of 48.8 s. Hence, the probability of failure is lower outside the time interval of 17.2 h mentioned above.

8. Summary and conclusions

The impact of data uncertainties on the prediction of the dynamic behaviour of a typical exothermal process is shown. Considerable differences as compared with the conventional calculations based on point values result. These should be considered in both, in design and safety calculations.

Two methods for the propagation of uncertainties through the calculations are presented, Monte-Carlo and polynomial chaos. The difference in computing time is more than two orders of magnitude. Therefore the polynomial chaos approach is to be preferred, especially if many parameter variations are required as, for example, in the case of calculating the time available for a reactor trip by dumping.

However, it should be borne in mind that the conceptual simplicity makes Monte-Carlo much easier to implement, which may be a criterion for its choice. Additionally, the advantage of polynomial chaos may dwindle if there are too many uncertain quantities involved or the deviation from Gaussian behaviour is too strong.

References

- [1] G.M. Morgan, M. Henrion, *Uncertainty—A Guide to Dealing with Uncertainty in Quantitative Risk and Policy Analysis*, Cambridge University Press, New York, 1990.
- [2] S. Balakrishnan, P. Georgopoulos, I. Banerjee, M. Ierapetriou, Uncertainty considerations for describing complex reaction systems, *AIChE J.* 48 (12) (2002) 2875–2889.
- [3] N. Watanabe, Y. Nishimura, M. Matsubara, Optimal design of chemical processes involving parameter uncertainty, *Chem. Eng. Sci.* 28 (1973) 905–913.
- [4] N. Nishida, A. Ichikawa, E. Tazaki, Synthesis of optimal process systems with uncertainty, *Ind. Eng. Chem. Process Des. Dev.* 13 (1974) 209–214.
- [5] R. Henrion, P. Li, A. Möller, M.C. Steinbach, M. Wendt, G. Wozny, *Stochastic optimization for operating chemical processes under uncertainty*, ZIB-Report 01-04, Konrad-Zuse-Zentrum für Informationstechnik, Berlin, 2001.
- [6] T. Knetsch, U. Hauptmanns, Integration of stochastic effects and data uncertainties into the design of process equipment, *Risk Anal.* 25 (1) (2005) 189–198.
- [7] U. Hauptmanns, Uncertainty and the calculation of safety-related parameters for chemical reactions, *J. Loss Prev. Process Ind.* 10 (4) (1997) 243–247.
- [8] U. Hauptmanns, Boundary conditions for developing a safety concept for an exothermal reaction, *J. Hazard. Mater.* 148 (2007) 144–150.
- [9] B.D. Ripley, *Stochastic Simulation*, John Wiley & Sons, New York, 1987.
- [10] N. Wiener, The homogeneous chaos, *Am. J. Math.* 60 (1938) 897–936.
- [11] R.G. Ghanem, P.D. Spanos, *Stochastic Finite Elements: A Spectral Approach*, Springer-Verlag, New York, 1991.
- [12] M.T. Reagan, H.N. Naim, P.P. Pébay, O.M. Knio, R.G. Ghanem, Quantifying uncertainty in chemical systems modelling, *Int. J. Chem. Kinet.* 37 (6) (2005) 368–382.
- [13] M.T. Reagan, H.N. Naim, B.J. Debusschere, O.P. Le Maître, O.M. Knio, R.G. Ghanem, Spectral stochastic uncertainty quantification in chemical systems, *Combust. Theory Model.* 8 (3) (2004) 607–632.
- [14] T. Urbanski, *Chemistry and Technology of Explosives*, Pergamon Press, Oxford, New York, 1965–1967.
- [15] K.-M. Luo, S.-H. Lin, J.-G. Chang, T.-H. Huang, Evaluations of kinetic parameters and critical runaway conditions in the reaction system of hexamine-nitric acid to produce RDX in a non-isothermal batch reactor, *J. Loss Prev. Process Ind.* 15 (2002) 119–127.

- [16] K.R. Westerterp, W.P.M. van Swaaij, A.A.C.M. Beenackers, *Chemical Reactor Design and Operation*, John Wiley & Sons, Chichester, July 1995.
- [17] N.L. Johnson, S. Kotz, N. Balakrishnan, *Continuous Univariate Distributions*, vols. 1 and 2, John Wiley & Sons, New York, 1995.
- [18] J.E. Gentle, *Random Number Generation and Monte Carlo Methods*, Springer-Verlag, New York, 2003.
- [19] M. Abramowitz, I. Stegun, *Handbook of Mathematical Functions with Formulas, Graphs, and Mathematical Tables*, U.S. Department of Commerce, Washington, 1972.
- [20] D. Xiu, G.E. Karniadakis, The Wiener–Askey polynomial chaos for stochastic differential equations, *SIAM J. Sci. Comput.* 24 (2) (2002) 619–644.
- [21] R.H. Cameron, W.T. Martin, The orthogonal development of nonlinear functionals in series of Fourier-Hermite functionals, *Ann. Math.* 48 (2) (1947) 385–392.
- [22] D. Lucor, G.E. Karniadakis, Adaptive generalized polynomial chaos for nonlinear random oscillators, *SIAM J. Sci. Comput.* 26 (2) (2004) 720–735.
- [23] H.A.R. Barnett, The variance of the product of two independent variables and its application to an investigation based on sample data, *J. Inst. Actuaries* 81 (1955) 190.